Variation Source Identification in Manufacturing Processes Based on Relational Measurements of Key Product Characteristics

Jean-Philippe Loose
e-mail: jploose@wisc.edu

Shiyu Zhou
e-mail: szhou@engr.wisc.edu

Dariusz Ceglarek
e-mail: D.J.Ceglarek@warwick.ac.uk

Department of Industrial and Systems Engineering,
University of Wisconsin-Madison,
Madison, Wisconsin 53706; and
Warwick Digital Laboratory,
University of Warwick,
Coventry, CV4 7AL, United Kingdom

Variation source identification for manufacturing processes is critical for product dimensional quality improvement, and various techniques have been developed in recent years. Most existing variation source identification techniques are based on a linear fault-quality model, in which the relationships between process faults and product dimensional quality measurements are linear. In practice, many dimensional measurements are actually nonlinearly related to the process faults: For example, relational dimension measurements such as the relative distance between features are used to monitor composite tolerances. This paper presents a variation source identification methodology in the presence of these relational dimension measurements. In the proposed methodology, the joint probability density of the measurements is determined as a function of the process parameters; then, series of statistical comparisons are performed to differentiate and identify the variation source. A case study is also presented to illustrate the effectiveness of the methodology. [DOI: 10.1115/1.2844591]

Keywords: relational dimension measurements, quality control, variation source identification

1 Introduction

The ability to detect and reduce variation in manufacturing gives competitive advantages to companies today, allowing them to provide better quality products to their customers. Traditional quality control in manufacturing focuses on statistical process control (SPC) to detect anomalies based on product and process measurements. However, this approach does not provide guidelines to identify the variation source, a critical step toward variation reduction. The concept of variation source is illustrated for an assembly operation in which two parts are welded together (Fig. 1). In Fig. 1, a solid line is used to represent positions of the parts constrained by fixture locators at the nominal design, and a dashed line is used to represent the actual positions of the parts and fixture elements. Figure 1(*a*) shows the final product as designed. The assembly process is as follows: Part 1 is first located on the fixture and constrained by four-way Pin L_1 and two-way Pin L_2. Then, Part 2 is located by four-way Pin L_3 and two-way Pin L_4. The two parts are then welded together in a joining operation and released from the fixture. If Pin L_1's position or diameter deviates from the nominal design, then, consequently, Part 1 will not be in its nominal design position, as shown in Fig. 1(*b*). After joining Parts 1 and 2, the final part's dimensions will deviate from the designed nominal values. In this example, mislocations of the locating pin can be manifested by mean shift or variance change in the measurement data due, for example, to errors in the design or the setup of the fixture. In the case of mean shift error, the error can be compensated by process adjustment, for example, by lowering Pin L_3 to align Part 2 with Part 1. The variance change error can be caused by a variation of the location of Pin L_1, for example, due to pin worn-out or the excessive looseness of that pin. The variance change error causing an excessive variation of process parameters, called "variation source," cannot be easily compensated for in most of the cases, unless adaptive assembly capability exists.

In most of the cases, the variation change can be detected by SPC schemes; however, the variation source cannot be identified using traditional SPC techniques. Moreover, the complexity of modern manufacturing processes used in automotive, aerospace, or electronic industries makes it very difficult to efficiently identify the variation sources based solely on the operators' knowledge and experience. For example, a typical automotive body assembly process consists of 150–250 parts, with 55–75 stations [1]. On the other hand, the development of a new sensor technology allows deployment of end-of-line or distributed measurement stations, which can measure up to 100% of assembled products. For instance, a 100% dimensional inspection has been achieved for an automotive assembly process using inline optical coordinate measurement machines (OCMMs) [1]. The availability of product and process measurement data as well as the criticality of problems caused by product variation led to the significant development of new methodologies for variation source identification.

Extensive research and numerous variation source identification methodologies based on the following two assumptions have been conducted: (i) Measured product dimensional quality characteristics are critical to the assessment of the final product's functional requirements and assemblability. (ii) The relationship between the measured product dimensional quality characteristics and the process faults is linear, as shown by

$$\mathbf{Z} = \mathbf{A} \cdot \mathbf{u} + \boldsymbol{\varepsilon} \tag{1}$$

In this equation, $\mathbf{Z}$ is a $(m \times 1)$ random vector representing the product quality measurements, $\mathbf{u}$ is a $(n \times 1)$ random vector representing the variation sources, $\mathbf{A}$ is a $(m \times n)$ design matrix determined by the product and process information, and $\boldsymbol{\varepsilon}$ is the term capturing the random noise in the process. For example, in the assembly process shown in Fig. 1, the deviations of the locating pins in the direction of x and y are variation sources. In this example, there are $n=8$ possible variation sources and $\mathbf{u}$

Contributed by the Manufacturing Engineering Division of ASME for publication in the JOURNAL OF MANUFACTURING SCIENCE AND ENGINEERING. Manuscript received October 6, 2006; final manuscript received January 2, 2008; published online May 6, 2008. Review conducted by Shivakumar Raman.

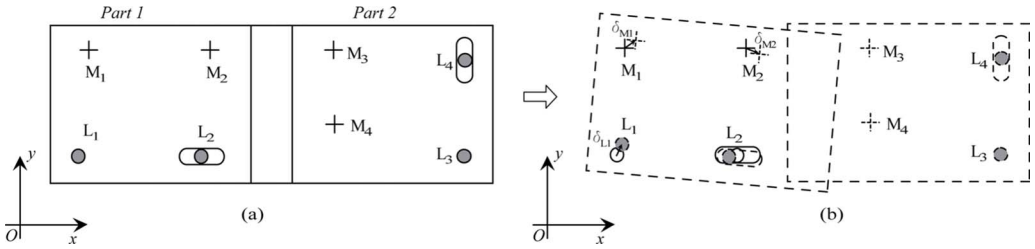

Fig. 1 Variation source in an assembly operation

$=[\boldsymbol{\delta}_{L1}^T\ \boldsymbol{\delta}_{L2}^T\ \boldsymbol{\delta}_{L3}^T\ \boldsymbol{\delta}_{L4}^T]^T$, where $\boldsymbol{\delta}_{L1}=[\delta_{L1,x}\ \boldsymbol{\delta}_{L1,y}]^T$, with $\boldsymbol{\delta}_{L1,x}$ corresponding to the deviation of Pin L_1 in the x direction. Furthermore, the deviations of the measured points (M_1, M_2, M_3, and M_4) are captured in the product quality vector $\mathbf{Z}$. In this example, there are $m=8$ measurements and $\mathbf{Z}=[\boldsymbol{\delta}_{M1}^T\ \boldsymbol{\delta}_{M2}^T\ \boldsymbol{\delta}_{M3}^T\ \boldsymbol{\delta}_{M4}^T]^T$, where $\boldsymbol{\delta}_{M1}=[\delta_{M1,x}\ \delta_{M1,y}]^T$, with $\delta_{M1,x}$ corresponding to the deviation of point M_1 in the x direction. The variation source identification involves the identification of matrix $\mathbf{A}$ and the estimation of the variances of the elements of $\mathbf{u}$ based on $\mathbf{A}$ and observations of $\mathbf{Z}$.

Currently available variation source identification methodologies based on Eq. (1) can be classified into analytical and data-driven approaches. The analytical approaches rely on the use of analytical fault-quality models developed based on physical knowledge of the process. In other words, matrix $\mathbf{A}$ from Eq. (1) is obtained through engineering analysis of the product and process designs. Then, pattern-matching methods or direct estimation methods are used to estimate the variation sources. For example, Ceglarek and Shi [2] proposed a pattern-matching variation source identification methodology based on principal component analysis. This method was extended by Ding et al. [3] for a single fault diagnosis of multistage assembly processes. Also, Ceglarek and Shi [4], Li et al. [5], and Li and Zhou [6] extended the pattern-matching method to the cases where measurement noise is unstructured and multiple faults occur simultaneously in the process. Ding et al. [7] and Zhou et al. [8] studied the diagnosability of multistage manufacturing processes based on the theory of linear mixed-effect model. Zhou et al. [9] used a maximum likelihood estimator and discussed the confidence interval of the estimated results. Huang and Shi [10] proposed a variational analysis method for multistage manufacturing processes. The one-dimension relational measurements that are linear to the system fault are considered in their work. A comparative analysis of various estimation methods is presented in Ding et al. [11].

In the data-driven approaches, model matrix $\mathbf{A}$ is estimated using available historical observations of $\mathbf{Z}$. Apley and Shi [12] and Apley and Lee [13] proposed methodologies to estimate the model matrix based on factor analysis and independent component analysis, respectively. Most recently, Jin and Zhou [14,15] proposed a procedure for self-improving data-driven variation source identification based on principal component analysis in the case where multiple faults occur in the process.

In both analytical and data-driven approaches, the measured product quality characteristics are based on direct measurements of the individual key characteristics represented as individual points that deviated from the nominal design or based on linear combinations of point deviations. When the magnitude of process fault is small, the relationship between the deviations of the individual points and the process faults can often be well approximated as linear, as shown with the linear formulation of Eq. (1). These quality characteristics' measurements based on individual points are called linear measurements.

However, in practice, these linear measurements might not be sufficient to represent the intended function for which the product was designed. Instead, relational product quality characteristics, critical to the product intended function, might be measured and monitored. The concept of relational product quality characteristic is illustrated in Fig. 2 for a hinge.

In Fig. 2, the tolerances on the two holes of a hinge are represented following the geometric dimensioning and tolerancing (GD&T) standards [16]. Such tolerances are called "composite" since one hole's positional tolerance is constrained by another hole, which has its own positional tolerance. The critical product characteristic in this example is the relative position of one hole with respect to the other. This product characteristic is critical to the function of the hinge to locate two pieces accurately with respect to each other when allowing rotation between them. However, the position of the holes with respect to their housing does not matter to this function.

Based on these examples, we can define a linear product characteristic as a product characteristic solely based on individual point deviations. Also, we can define a relational product characteristic as a product characteristic not solely based on individual point deviation, but rather on relations between points, features, or multiple other product characteristics. In practice, the relational product characteristic is often *nonlinearly* related to the corresponding linear characteristics. For example, the relational product characteristic of the hinge in Fig. 2 is the distance between the two holes, which is nonlinearly related to the absolute positions of these two holes. Although the measurement of relational characteristic can be obtained by measuring the position of individual points (i.e., the corresponding linear characteristic), followed by a calculation of the relational characteristic, it is often obtained and reported through direct measuring in practice, particularly when hard gauging is used. Thus, how to utilize the relational measurements for variation source identification is an important engineering problem.

Current methodologies for variation source identification only consider linear measurements. In this paper, we investigate the variation source identification methodology when both linear and relational measurements are available. The general model can be represented as

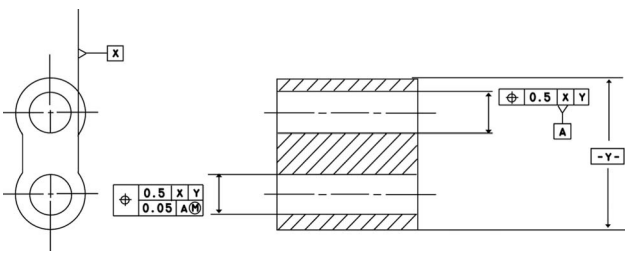

Fig. 2 Engineering drawing for a hinge illustrating relational quality characteristics

$$\mathbf{Z} = \mathbf{F}(\mathbf{A} \cdot \mathbf{u}) + \boldsymbol{\varepsilon} \tag{2}$$

where $\mathbf{u}$ is a $(n \times 1)$ random vector, which represents the process faults, $\mathbf{A}$ is a known matrix obtained from the engineering analysis of the process, $\mathbf{Z}$ is a $(m \times 1)$ random vector of the product quality characteristics measured during the inspection process, $\boldsymbol{\varepsilon}$ is a $(m \times 1)$ random vector capturing the random noise in the measurement process, and $\mathbf{F}$ is a vector of vector functions and will be discussed in detail in Sec. 2. The goal of the proposed methodology is to systematically identify the components of $\mathbf{u}$ that has a large variance based on the known matrix $\mathbf{A}$, function $\mathbf{F}$, and observations of quality measurements $\mathbf{Z}$.

The paper is organized as follows: In Sec. 2, a mathematical formulation of the problem is provided and the overall methodology is outlined. Section 3 presents the details of each step of the proposed methodology. An industrial case study illustrates the methodology in Sec. 4. Section 5 discusses the robustness of the methodology with respect to the assumptions. Finally, conclusions and future work are discussed in Sec. 6.

2 Problem Formulation

In this section, we first formulate the problem mathematically and present the assumptions of the proposed methodology. Then, the overall methodology is outlined.

2.1 Mathematical Formulation. We assume that a known fault-quality model that links the quality characteristics of the workpiece $\mathbf{Z}$ and the process parameters $\mathbf{u}$ exists, as expressed in Eq. (2). In this model, the vector of vector functions $\mathbf{F}$ is general and can be expressed as

$$\mathbf{F}(\cdot) = [f_1(\cdot) \quad \cdots \quad f_m(\cdot)]^T \tag{3}$$

where $f_k(\cdot): \Re^n \rightarrow \Re$ represents a vector function $(k=1, \ldots, m)$ and m represents the dimension of the measurement vector $\mathbf{Z}$. If all the functions $f_k(\cdot)$ are linear for all $k=1, \ldots, m$, then Eq. (2) is simplified to Eq. (1). However, as highlighted in the Introduction, in many cases, function $f_k(\cdot)$ is nonlinear, for example, when describing relational product characteristics such as (a) 2D distances between points, (b) 3D distances between features, and (c) minimum and maximum variations of the profile of a feature.

In this paper, for the sake of simplicity, the developed methodology will be discussed by using the functions representing distances. However, the presented methodology is general and can be applied to other functions as well. Without loss of generality, we assume that the first p measurements are linear measurements and the next $(m\text{-}p)$ measurements are distance measurements taken in the process.

Denoting as $\mathbf{A}_k$ the kth row of design matrix $\mathbf{A}$ the overall model described by Eq. (2) can be written as

$$[Z_1 \quad \cdots \quad Z_p \quad Z_{p+1} \quad \cdots \quad Z_m]^T = [\mathbf{A}_1 \cdot \mathbf{u} \quad \cdots \quad \mathbf{A}_p \cdot \mathbf{u} \quad f_{p+1}(\mathbf{A} \cdot \mathbf{u}) \quad \cdots \quad f_m(\mathbf{A} \cdot \mathbf{u})]^T + \boldsymbol{\varepsilon} \tag{4}$$

As mentioned earlier, the nonlinear functions represent distances between points on the workpiece: Given two points on parts P_1 and P_2, we define the distance between these two points as

$$Z = \text{dist}(P_1, P_2) = \sqrt{(P_{1x} - P_{2x})^2 + (P_{1y} - P_{2y})^2 + (P_{1z} - P_{2z})^2} \tag{5}$$

where (P_{1x}, P_{1y}, P_{1z}) and (P_{2x}, P_{2y}, P_{2z}) represent the coordinates of points P_1 and P_2, respectively, and can be expressed as a linear function of the process variation sources $\mathbf{u}$ as

$$\mathbf{P}_i = [P_{ix} \quad P_{iy} \quad P_{iz}]^T = [\mathbf{A}_{P_{ix}} \cdot \mathbf{u} \quad \mathbf{A}_{P_{iy}} \cdot \mathbf{u} \quad \mathbf{A}_{P_{iz}} \cdot \mathbf{u}]^T \tag{6}$$

Then, the complete model expressed in Eq. (2) can be represented as

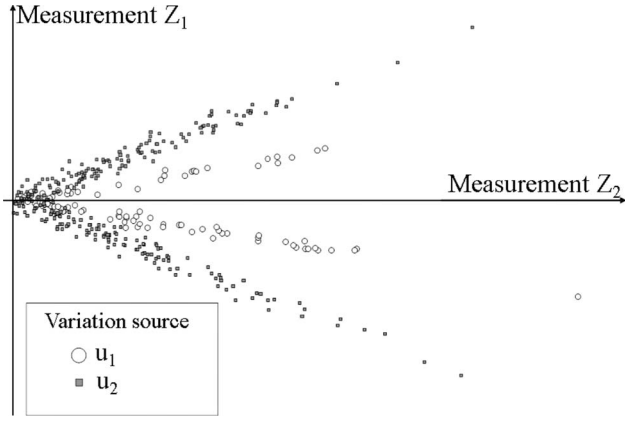

Fig. 3 Illustration of the inefficiencies of PC as patterns for variation source identification

$$Z_k = \mathbf{A}_k \cdot \mathbf{u} + \varepsilon_k, \quad k = 1, \ldots, p$$

$$Z_k = \text{dist}(P_{i,k}, P_{j,k}) + \varepsilon_k, \quad k = (p+1), \ldots, m \tag{7}$$

where i and j are indices for points on the workpiece. Equation (7) shows the general model expressed for p linear measurements and $(m\text{-}p)$ distance measurements.

The current available variation source identification methodologies cannot utilize the distance measurements to identify the variation sources. Traditional pattern-matching methodologies are based on the following fact: If Eq. (1) holds, the eigenvectors of $\Sigma_{\mathbf{Z}}$ (the covariance matrix of $\mathbf{Z}$) that are associated with large eigenvalues span the same linear space as the column vectors of model matrix $\mathbf{A}$ associated with the faulty components of $\mathbf{u}$ (i.e., components with large variances). Thus, if $\mathbf{A}$ is known, by comparing its columns with the eigenvectors of $\Sigma_{\mathbf{Z}}$, we can identify which components of $\mathbf{u}$ are at fault. However, the following example shows that, given two distinct variation sources, the eigenvectors of $\Sigma_{\mathbf{Z}}$ are very close from each other; further, the example shows that the eigenvectors are highly unstable if distance measurements are included in the pattern-matching procedure.

In this example, we assume one linear measurement Z_1 and one distance measurement Z_2 (corresponding to the distance between points P_1 and P_2) and two possible variance sources, namely, u_1 and u_2. Principal components are used for variation source identification. For this example, we have

$$\mathbf{A} = \begin{bmatrix} 0.6 & 1 & 0 & 0.2 & 0 \\ 0.9 & 0 & 1 & 0 & 0.5 \end{bmatrix}^T$$

with the first row corresponding to the linear measurements, the second and third rows corresponding to the position of point P_1 in the x and y directions, and the fourth and fifth rows corresponding to the position of point P_2 in the x and y directions. Therefore, Eq. (7) can be expressed as

$$Z_1 = 0.6u_1 + 0.9u_2 + \varepsilon_1$$

$$Z_2 = \sqrt{0.64u_1^2 + 0.25u_2^2} + \varepsilon_2 \tag{8}$$

Figure 3 shows the plot of linear measurement Z_1 versus relational measurement Z_2. The points marked as circles correspond to the case where the variation source is u_1; the points marked as squares correspond to the case where the variation source is u_2.

Simulations of these two cases, where u_1 and u_2 are the variation sources, respectively, have been conducted, assuming that u_1, u_2, ε_1, and ε_2 are independently identically distributed (iid) following a normal distribution with mean 0 and variance 2, 3, 0.1, and 0.1, respectively. The simulation has been carried out 1000 times for 300 samples for each case; the results show that the

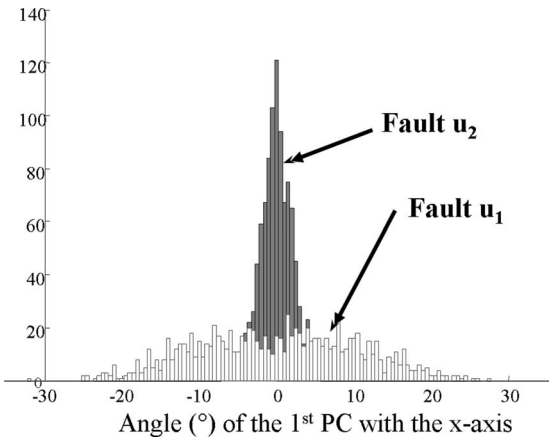

Fig. 4 Distribution of the angle between the first PC and the *x* axis

eigenvector associated with the largest eigenvalue are very close to each other in these two cases, with a mean angle of 0.6797 deg between them. This implies that the two variation sources cannot be differentiated using pattern-matching method. Also, the simulation shows that the angle between the eigenvector associated with the largest eigenvalue and the x axis has a very large variance. As shown in Fig. 4, the eigenvector is very unstable: The standard deviation of the angle of the first PC to the x axis of the measurements given that fault u_1 occurs is 10.31 deg. This implies that the eigenvector cannot be used as a meaningful pattern for variation source identification in this case.

As shown with this example, current methodologies cannot be applied in the presence of the distance measurements. In the following, the new methodology for variation source identification including both linear and relational measurements under the assumption that a single fault occurs is presented in detail. The assumption that a single fault occurs implies that a single element in $\mathbf{u}$ has a large variance and is the major contributor to the product dimensional quality. This assumption is widely accepted in the literature [2,17], and is not restrictive in practice, given the small probability of a fault happening in the system.

2.2 Methodology for Variation Source Identification Using Relational Product Characteristics. Equation (7) will be used as the underlying model for the proposed variation source identification. The general methodology is presented in this section. The overall methodology consists of the generation of a distribution function library, each distribution function in the library corresponding to a unique variation source; then, given product quality measurements, a statistical comparison is used to verify which distribution function provides the best fit to the data; the variation source corresponding to the distribution function providing the best fit to the data will be claimed to have occurred in the process. The general procedure is presented in Fig. 5. Each of the steps is outlined in the following paragraphs and is detailed in Sec. 3.

Step 1. In the first step, the model presented in Eq. (7) is simplified based on the assumption that no multiple variation source exists simultaneously in the system. This step is repeated for each variation source, and a set of n nonlinear models linking the product quality characteristics with the variation source is obtained, each corresponding to a single variation source. The single variation source assumption ensures that the magnitude of the variance of the component of $\mathbf{u}$ corresponding to the process fault is much larger than the variances of all other components.

Step 2. For each of the n models obtained in the first step, the multivariate joint probability density function (pdf) of all linear and relational measurements is derived. In order to derive the joint pdfs, the noise will be assumed to be independent of the variation source. In this step, a library of distribution functions is created, each element corresponding to a pdf assuming the realization of one process fault.

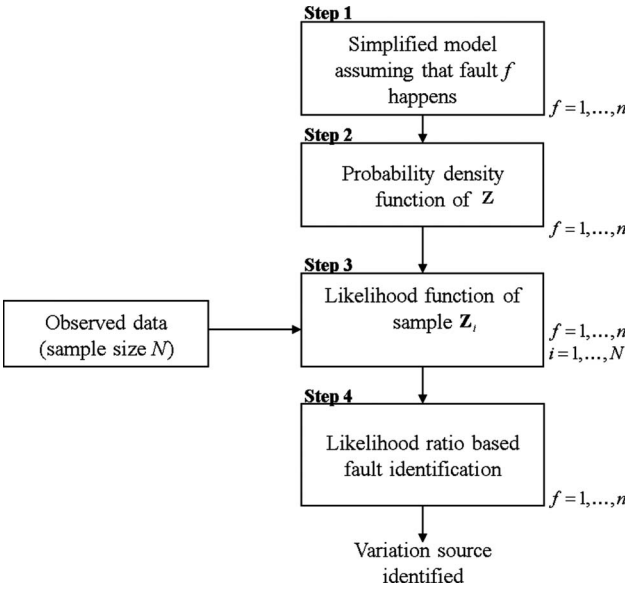

Fig. 5 Steps for the variation source identification including relational measurements

Step 3. Based on the functions obtained in Step 2, and given the data collected from the process and products, the likelihood functions of the data are calculated.

Step 4. In this final step, a statistical procedure is used to decide which variation source occurred in the system. A ratio of likelihood functions is used for this purpose: A set of n simultaneous independent comparisons is performed, and the criteria to determine which fault occurred in the system likelihood ratio is used as a test.

The details of these four steps are presented in Sec. 3.

3 Variation Source Identification Using Nonlinear Relations

3.1 Model Simplification. In this section, we present the procedure to simplify Eq. (7) under the assumption that only one fault occurs in the process; under normal working conditions, the process variables $\mathbf{u}$ are assumed to be normally distributed with zero mean and covariance matrix $\Sigma_{\mathbf{u}}=\sigma^2\cdot\mathbf{I}_n$, where σ^2 is the variance of the process parameters and n represents the number of variation sources. If the fth fault, called fault f, occurs, the corresponding element of $\mathbf{u}$ is assumed to be normally distributed with zero mean and σ_f^2, with $\sigma_f^2\gg\sigma^2$. Also, we assume that the measurement noise $\boldsymbol{\varepsilon}$ is normally distributed with mean 0 and covariance matrix $\Sigma_\varepsilon=\sigma_\varepsilon^2\cdot\mathbf{I}_m$, where σ_ε^2 is the variance of the noise and m represents the number of measurements. The assumption of independence of the noise from the variation sources has been commonly used in existing variation source identification [2,17–19] and validated in practice since most measuring systems do not influence the manufacturing process.

If fault f occurs in the system, Eq. (7) can be rewritten as

$$Z_k^f = a_{k,f}u_f + \varepsilon_k, \quad k=1,\ldots,p$$

$$Z_k^f = \sqrt{(a_{P_{ix},f}-a_{P_{jx},f})^2+(a_{P_{iy},f}-a_{P_{jy},f})^2+(a_{P_{iz},f}-a_{P_{jz},f})^2}|u_f|+\varepsilon_k = b_{k,f}\cdot|u_f|+\varepsilon_k, \quad k=(p+1),\ldots,m \tag{9}$$

where $a_{i,j}$ corresponds to the element on the ith row and the jth column of the model matrix $\mathbf{A}$ and $|\cdot|$ is the absolute value function. Because the measure of a distance is always positive, we

have $Z_k^f \geq 0$ for $k=(p+1),\ldots,m$. Therefore, $Z_k^f=|Z_k^f|$ and Eq. (9) can be represented as

$$Z_k^f = a_{k,f}u_f + \varepsilon_k, \quad k=1,\ldots,p$$

$$Z_k^f = |b_{k,f}|u_f| + \varepsilon_k|, \quad k=(p+1),\ldots,m \tag{10}$$

To simplify the notation in the remaining of the paper, we introduce the constant matrix $\mathbf{C}$ defined such that the fth column $\mathbf{C}_f$ of $\mathbf{C}$ gathers the parameters corresponding to the simplified model in Eq. (10) given the assumption that fault f occurs in the process; all parameters of $\mathbf{C}$ are known from the components of model matrix $\mathbf{A}$.

$$\mathbf{C} = [\mathbf{C}_1 \quad \cdots \quad \mathbf{C}_n] = \begin{bmatrix} a_{1,1} & \cdots & a_{1,n} \\ \vdots & \ddots & \vdots \\ a_{p,1} & \cdots & a_{p,n} \\ b_{p+1,1} & \cdots & b_{p+1,n} \\ \vdots & \ddots & \vdots \\ b_{m,1} & \cdots & b_{m,n} \end{bmatrix}$$

For each possible fault $f=(1,\ldots,n)$, the measurements assuming that fault f occurs can be expressed as a function of the process parameters in an integrated simplified model,

$$\mathbf{Z}^f = [C_{1,f}u_f + \varepsilon_1 \quad \cdots \quad C_{p,f}u_f + \varepsilon_p \quad |C_{p+1,f}|u_f| + \varepsilon_{p+1}| \quad \cdots \quad |C_{m,f}|u_f| + \varepsilon_m|] \tag{11}$$

where $C_{i,j}$ corresponds to the elements on the ith row and the jth column of the constant matrix $\mathbf{C}$.

3.2 Joint Probability Density Function of the Measurements Assuming Fault *f*. In this step, the multivariate joint pdf of $\mathbf{Z}^f$ is derived from Eq. (11) obtained in Step 1. $\mathbf{Z}^f$ is a set of m random variables. The joint cumulative density function of $\mathbf{Z}^f$ denoted as $G^f(\mathbf{Z}^f)$, is given by

$$G^f(\mathbf{Z}^f) = P\{\mathbf{Z}^f \leq \mathbf{z}\} = P\{\mathbf{Z}_1^f \leq z_1, \ldots, \mathbf{Z}_m^f \leq z_m\} \tag{12}$$

Equation (12) can be rewritten as Eq. (13) by partitioning the space for $u_f>0$ and $u_f<0$, where u_f is the component of $\mathbf{u}$ corresponding to the process fault f,

$$G^f(\mathbf{Z}^f) = P\{\mathbf{Z}^f \leq \mathbf{z} \text{ when } u_f > 0\} + P\{\mathbf{Z}^f \leq \mathbf{z} \text{ when } u_f < 0\} \tag{13}$$

Based on the constant matrix $\mathbf{C}$ defined in Step 1, on the two conditions $u_f>0$ and $u_f<0$ highlighted in Eq. (13), and on the assumption that $\boldsymbol{\varepsilon}$ is normally distributed with mean 0 and covariance matrix $\boldsymbol{\Sigma}_\varepsilon=\sigma_\varepsilon^2\cdot\mathbf{I}_m$, Eq. (11) can be decomposed into a set of equations as in Table 1.

In Table 1, it is shown that although the system is nonlinear overall, the simplified model is piecewise linear: The system of equations shown creates a partition of the space of $\mathbf{u}$ and $\boldsymbol{\varepsilon}$, denoted as Φ, into $2^{(m-p+1)}$ regions Φ_r $(r=1,\ldots,2^{(m-p+1)})$, and the relationship between the quality measurements and the process fault is linear in each region. To provide an intuitive understanding of these partitions, an example is shown in Fig. 6 for the system introduced in Sec. 2. In this example, two measurements were taken, one linear and one nonlinear, $\mathbf{Z}_1$ and $\mathbf{Z}_2$, respectively, and there were two possible variation sources $\mathbf{u}_1$ and $\mathbf{u}_2$. The partition of the space when $\mathbf{u}_1$ occurs is shown in Fig. 6.

In this example, for $k=1$ (e.g., for the linear measurement), the space $(u_1,\varepsilon_1,\varepsilon_2)$ is not partitioned, as expected. For $k=2$ (e.g., for the nonlinear measurement), the space is partitioned into four regions (denoted as 1–4 in Fig. 6) separated by the half-plane $(\varepsilon_2=-0.9u_1)$ for $u_1>0$ and by the half-plane $(\varepsilon_2=0.9u_1)$ for $u_1<0$.

With each region Φ_r being identified, the joint density of $\mathbf{Z}^f$ can be calculated on the entire space Φ as

$$G^f(\mathbf{Z}^f) = \sum_{\Phi} (P\{\mathbf{Z}^f \leq \mathbf{z} | u_f \in \Phi_r\}) = \int_{\Phi} g(u_f,\varepsilon_1,\ldots,\varepsilon_m) \tag{14}$$

where $g(u_f,\varepsilon_1,\ldots,\varepsilon_m)$ is the joint probability function of the $m+1$ random variables $u_f,(\varepsilon_k)_{k=1,\ldots,m}$; because all the regions Φ_r constitute the full space Φ, the cumulative density function can be determined by successive integration as shown in

$$G^f(\mathbf{Z}^f) = \int_{u_f=-\infty}^{\infty} \left(\int_{\varepsilon_1=-\infty}^{(z_1-C_{1,f})} \cdots \int_{\varepsilon_p=-\infty}^{(z_p-C_{p,f})} \int_{\varepsilon_{p+1}=-(z_{p+1}+C_{p+1,f})}^{(z_{p+1}-C_{p+1,f})} \cdots \int_{\varepsilon_m=-(z_m+C_{m,f})}^{(z_m-C_{m,f})} g(u_f,\varepsilon_1,\cdots,\varepsilon_m) dz_1 \cdots dz_m \right) \tag{15}$$

The assumption of independence of the measurement noise leads to the simplification of the joint pdf $g(u_f,\varepsilon_1,\ldots,\varepsilon_m)$ using

$$g(u_f,\varepsilon_1,\ldots,\varepsilon_m) = g_0(u_f)g_1(\varepsilon_1)\cdots g_m(\varepsilon_m) \tag{16}$$

where $g_0(\cdot),g_1(\cdot),\ldots,g_m(\cdot)$ are the marginal pdfs of $u_f,\varepsilon_1,\ldots,\varepsilon_m$. Furthermore, since both process variable $\mathbf{u}$ and noise $\boldsymbol{\varepsilon}$ are assumed to be normally distributed and centered, their pdfs are determined by

$$g_0(X) = \cdots = g_m(X) = \frac{1}{\sqrt{2\pi}} e^{-X^2/2\sigma^2} \tag{17}$$

where σ^2 is the variance of the variable X of interest.

From Eqs. (11) and (15)–(17), the pdf of $\mathbf{Z}^f$ is determined as

$$g^f(\mathbf{Z}^f) = \frac{e^{-(\mathbf{Z}^{fT}\mathbf{Z}^f/(2\sigma_\varepsilon^2))}}{\pi^{m/2}\sigma_\varepsilon^{m-1}2^{(m-2p)/2+1}\sqrt{\sigma_\varepsilon^2+\sigma_f^2\cdot\mathbf{C}_f^T\mathbf{C}_f}} \times \sum_{k=1}^{2^{m-p}} e^{((\sigma_f^2\cdot\mathbf{S}_k\cdot\mathbf{B}\cdot\mathrm{diag}(\mathbf{C}_f)\cdot\mathbf{Z}^f)^2/(2\sigma_\varepsilon^2\sqrt{\sigma_\varepsilon^2+\sigma_f^2\cdot\mathbf{C}_f^T\mathbf{C}_f}))} \tag{18}$$

where $\mathbf{B}=[\mathbf{B}_1|\mathbf{B}_2]$, with $\mathbf{B}_1=(1)_{2^{m-p}\times p}$, $\mathbf{B}_2$ is a $(2^{m-p}\times(m-p))$ combinatory matrix. An illustration of a combinatory matrix is given by

$$\text{If } p=2 \text{ and } m=4, \text{ then } \mathbf{B}_2 = \begin{bmatrix} 1 & 1 \\ -1 & 1 \\ 1 & -1 \\ -1 & -1 \end{bmatrix} \tag{19}$$

The vector $\mathbf{S}_k$ is a $(2^{m-p}\times 1)$ selection vector where its kth component is the only nonzero component and is equal to 1, diag$(\cdot)$ corresponds to the operation transforming a $(m\times 1)$ vector

Table 1 Partition of the space and conditional equations

k	u_f	ε_k	Z_k^f
$k=(1,\ldots,p)$	$\forall u_f \in \Re$	$\forall \varepsilon_k \in \Re$	$Z_k^f=(C_{k,f}u_f+\varepsilon_k)$
$k=(p+1,\ldots,m)$	$u_f>0$	$\varepsilon_k>-C_{k,f}\cdot u_f$	$Z_k^f=(C_{k,f}u_f+\varepsilon_k)$
		$\varepsilon_k<-C_{k,f}\cdot u_f$	$Z_k^f=-(C_{k,f}u_f+\varepsilon_k)$
	$u_f<0$	$\varepsilon_k>C_{k,f}\cdot u_f$	$Z_k^f=(-C_{k,f}u_f+\varepsilon_k)$
		$\varepsilon_k<C_{k,f}\cdot u_f$	$Z_k^f=(C_{k,f}u_f-\varepsilon_k)$

into a $(m\times m)$ diagonal matrix, and $\mathbf{C}_f$ is the fth column of the constant matrix $\mathbf{C}$ defined in Step 1.

In the following, we present plots of the joint pdf, given different scenarios to illustrate the behavior of the function based on the example introduced in Sec. 2. In this example, $\mathbf{Z}_1$ refers to the linear measurement and $\mathbf{Z}_2$ refers to the relational measurement. Figure 7(*a*) illustrates the scenario when no fault occurs. The next three plots (Figs. 7(*b*)–7(*d*)) correspond to the scenarios when fault u_2 occurs with different magnitudes, characterized by a signal-to-noise ratio $(S/N_0=\sigma_{u_2}^2/\sigma_\varepsilon^2)$ equal to 3, 5, and 10 for Figs. 7(*b*)–7(*d*) respectively. Figure 7(*e*) shows the scenario when fault u_1 occurs with a signal-to-noise ratio of 5.

Insights about the behavior of the pdf can be drawn from Fig. 7. First, as we can see from all figures, the pdf is truncated; i.e., the probability is zero when $Z_2<0$; this is expected since the measure of a distance is always positive. Second, the distribution of Z_k^f for $k=1,\ldots,p$ is symmetric, i.e., the following condition is true:

$$\forall \mathbf{u}_0 \in \mathcal{R}, \quad P(Z_k^f \leqslant z_k | u_f = u_0) = P(Z_k^f \leqslant z_k | u_f = -u_0) \quad (20)$$

Therefore, it is expected that the pdf be symmetric with respect to the linear measurement of Z_1, as shown in Fig. 7. Third, from Fig. 7(*a*), we can see that when no fault happens, the multivariate pdf is simply a multivariate half-normal distribution associated with a normal distribution with mean 0 and covariance matrix $\Sigma_{\boldsymbol{\varepsilon}}=\sigma_\varepsilon^2\cdot\mathbf{I}_m$. This is expected since there is only noise in the system if no fault happens in the system. Fourth, from Figs. 7(*b*)–7(*d*), we can see the change in the shape of the pdf due to the fault, depending on the fault magnitude. Fifth, by comparing Figs. 7(*c*) and 7(*e*), we see that the shape of the pdf is different for each fault; in other words, the relative positions of the tails of the joint pdf depend on the parameters of matrix $\mathbf{C}$ introduced in Sec. 2. This implies that we can differentiate different faults by comparing the fit of observed measurements to the pdfs, given each fault scenario. This is actually the basic idea of the proposed variation source identification technique.

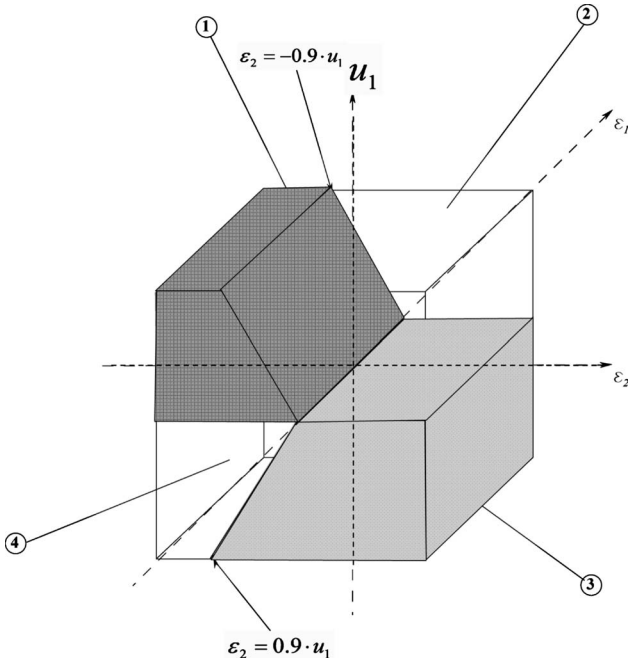

Fig. 6 Partition of the space for the example in Sec. 2 when u_1 is the variation source

3.3 Determination of the Likelihood Functions. Given quality measurements of sample size N, the likelihood function of the sample is defined as

$$L^f(\mathbf{C}_f,\sigma_f^2,\sigma_\varepsilon^2)=\left(\prod_{i=1}^{N} g^f(\mathbf{Z}_i)\right) \quad (21)$$

where $\mathbf{Z}_i$ corresponds to the ith measurement. The likelihood is a function of $m+2$ parameters $C_{1,f},\ldots,C_{m,f},\sigma_f^2,\sigma_\varepsilon^2$; $(C_{1,f},\ldots,C_{m,f})$ are known from the constant matrix $\mathbf{C}$ defined in Step 1. However, σ_f^2 and σ_ε^2 are unknown and need to be estimated to determine the value of the likelihood function. The variance of measurement noise can often be obtained from gauge R&R study [20]. In a typical assembly process, the noise variance is around 0.05 mm^2. A faulty condition is characterized by an increase of variance for a process variable. The threshold to define when a fault occurs (in other words, to define σ_f in Eq. (18)) is left at the practitioners' discretion: The closer the value is taken from the true fault variance shift, the better the result will be. A conservative way to estimate the variance shift of the fault is to use $\sigma_f^2=5\sigma_\varepsilon^2$. Alternatively, it is possible to calculate an estimate of the fault variance, given sample data as follows:

(a) Assume that fault f happens; then, find $j\leqslant p$ such that $\mathbf{C}_{j,f}\neq 0$, where $\mathbf{C}_{j,f}$ is the element on the jth row and the fth column of matrix $\mathbf{C}$.
(b) Determine the variance of the collected data for the jth measurement using

$$\hat{\sigma}_f^2=\frac{\text{Var}(\mathbf{Z}_j)-\hat{\sigma}_\varepsilon^2}{\mathbf{C}_{j,f}^2} \quad (22)$$

where $\hat{\sigma}_\varepsilon$ is the estimated variance of the noise.

The derivation of Eq. (22) is straightforward from the variance of a linear combination of normal random variables.

3.4 Likelihood Comparison for the Identification of the Variation Source. In this section, a likelihood comparison [21,22] procedure is used to identify the variation source. This comparison is used to examine whether a model provides a good fit to the sample data. We define the ensemble Θ_f, which contains all parameters of the model defined in Eq. (11): $\mathbf{C}_f$, σ_f, σ_ε. Also, we define the model ensemble for all n possible faults $\Theta=\cup_{k=1,\ldots,n}\Theta_k$ as the union of all ensembles of the individual fault models. When fault f occurs in the process, the best fit for the data is provided by the model with parameters from Θ_f; therefore, we perform a series of n simultaneous independent comparisons to identify the model that provides a good fit to the observed data.

For $i=1,\ldots,n$,

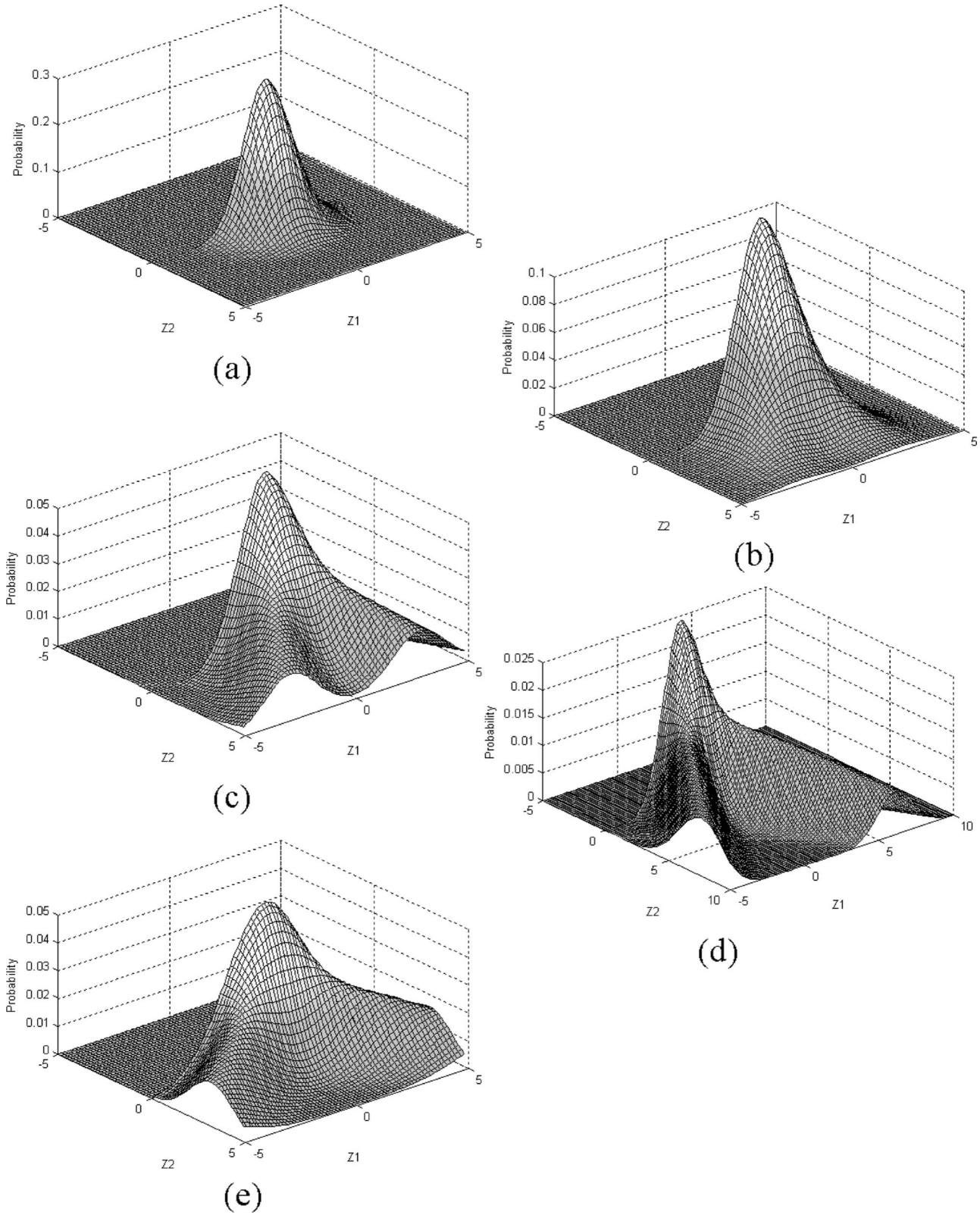

Fig. 7 Plots of the pdf, given different scenarios

$$\theta \in \Theta_i \quad \text{versus} \quad \theta \in \Theta/\Theta_i \tag{23}$$

where θ corresponds to the true parameters and Θ/Θ_i.

For each fault, the following ratio of likelihoods is determined,

$$\Lambda^i = -2\log\left(\frac{L^i(\mathbf{C}_i,\sigma_i^2,\sigma_\varepsilon^2)}{\sup_{j\neq i}(\mathbf{L}^j(\mathbf{C}_j,\sigma_j^2,\sigma_\varepsilon^2))}\right) \tag{24}$$

where sup(·) is the supremum function.

Given that the log function monotonically increases, Eq. (24) can be expressed using Eq. (21),

$$\Lambda^i = -2\sum_{t=1}^{N} \log[g^i(\mathbf{Z}_t^i)] + 2 \sup_{j\neq f}\left(\sum_{t=1}^{N} \log[g^j(\mathbf{Z}_t^j)]\right) \quad (25)$$

If fault f happens in the system, it is expected that $L^f(\mathbf{C}_f, \sigma_f^2, \sigma_\varepsilon^2) > \sup_{j\neq f}(\mathbf{L}^j(\mathbf{C}_j, \sigma_j^2, \sigma_\varepsilon^2))$, and therefore $\Lambda f < 0$. Thus, for $i=1,\ldots,n$, if $\Lambda i < 0$, the likelihood of fault i is the largest among all possible likeli

4 Case Study

4.1 Process Description. An industrial case study for an automotive assembly process is used to demonstrate the derivation of the models, the pdfs and the likelihood functions comparisons as discussed in this paper. Further, different scenarios for fault magnitudes and sample sizes are simulated to demonstrate the effectiveness of the proposed methodology.

The case study is based on a simplified process for automotive hood assembly (Fig. 8). The assembly consists of three stages involving the assembly of four parts. In the first stage, the right fender is assembled with the body; in the second stage, the left fender is assembled with the body; and in the last stage, the hood is assembled with the body and fenders. Figure 8 shows the subassemblies at the end of each station. In this process, there is a total of 27 locators among which four will be considered as potential variation sources.

The potential variation sources and quality measurements (points P_1-P_7) for the hood assembly process used in this simulation are shown in Fig. 9. The four locators L_1-L_4 under study are (1) deviation of locator L_2 in the y direction, (2) deviation of locator L_1 in the y direction, (3) deviation of locator L_3 in the x direction, and (4) deviation of locator L_4 in the z direction. In this assembly process, five product quality characteristics are critical and can be summarized as follows. (1) Linear product quality characteristics: deviation of point P_1 in the y direction, deviation of point P_2 in the x direction, and deviation of point P_3 in the y direction. (2) Relational product quality characteristics: distance between points P_4 and P_5 and distance between points P_6 and P_7. These relational product quality characteristics are observed in practice as they are critical both for the aesthetics of the hood and for the closing and sealing function of the hood.

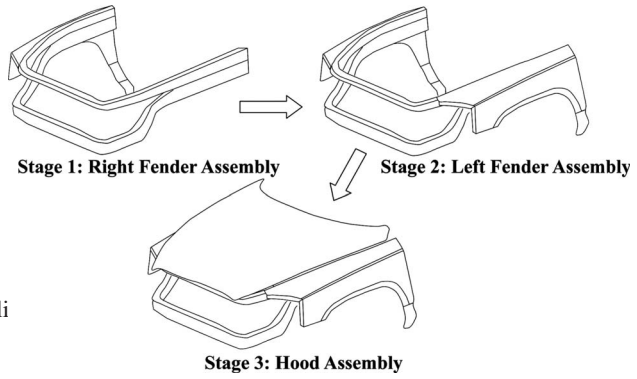

Fig. 8 Three step simplified hood assembly process

Through an engineering analysis, the linear relationship between the process faults and the locations of the seven points can be obtained [10,17,19,23–29]. Defining $\mathbf{Y}$ as a (15×1) vector of point locations and $\mathbf{u}$ (4×1) as the vector of process faults, where $Y(1)$ is the deviation of point P_1 in the y direction, $Y(2)$ is the deviation of point P_2 in the x direction, $Y(3)$ is the deviation of point P_3 in the y direction, $Y(4-6)$ are the deviations of point P_4 (on the Fender) in x-y-z-directions, $Y(7-9)$ are the deviations of point P_5 (on the Hood) in x-y-z-directions, $Y(10-12)$ are the deviations of point P_6 (on the Fender) in x-y-z-directions, and $Y(13-15)$ are the deviations of point P_7 (on the Hood) in x-y-z-directions, the corresponding model matrix $\mathbf{A}$ is

$$\mathbf{A} = \begin{bmatrix} -0.33 & 0 & 0 & 0 & 0 & 0 & 0 & 0.0675 & 0.0375 & 0 & 0.37 & 0 & 0 & 0.0675 & 0 \\ -0.33 & 0 & 0 & 0 & 0 & 0 & 0 & 0.7698 & 0 & 0.4 & 0.37 & 0.037 & 0 & 0.7698 & 0 \\ 0 & -1 & 0 & 0 & 0 & 0 & 0 & 0.3571 & 0 & -0.2 & 0 & 0.037 & 0 & 0.3571 & 0 \\ 0 & 0 & 1 & 0 & 1 & 0 & 0 & 0 & 0 & 0 & 1 & 0 & 0 & 0 & 0 \end{bmatrix}^T$$

It has to be pointed out that, in practice, the above mentioned five product quality characteristics are measured instead of the vector $\mathbf{Y}$.

4.2 Numerical Study. A single fault scenario is simulated in this case study corresponding to the failure of locator $L1$ in the y direction. Matrix $\mathbf{A}$ is used to generate the five measured product characteristics under different combinations of noise variance σ_ε^2, fault variance σ_f^2, and sample sizes N. The variance of the noise, σ_ε^2, take values from (0.01, 0.05, 0.1, 0.2). For each noise variance, the corresponding fault variance σ_f^2 is calculated so that the signal-to-noise (S/N_0) ratios, defined as $\sigma_f^2/\sigma_\varepsilon^2$, are 3, 5, and 10. Also, for each combination, cases of three different sample sizes N are generated ($N=20$, 50, and 100).

The methodology will be applied to two situations: (i) when only the linear measurements are considered for the variation source identification, and (ii) when all measurements including both linear and relational measurements are considered.

Step 1: Model simplification. For each possible variation source ($f=1,\ldots,4$), the column $\mathbf{C}_f$ is generated. For example, for $f=1$, $\mathbf{C}_1=[-0.33\ 0\ 0\ \sqrt{0.7689^2}\ \sqrt{0.4^2+(0.37-0.7698)^2+0.037^2}]^T$; thus,

$$\mathbf{C}_1 = [-0.33 \quad 0 \quad 0 \quad 0.7698 \quad 0.5668]^T \quad (26)$$

Step 2: Determination of the parameters of the pdf. Given $m=5$, the total number of measurements, and $p=3$, the number of linear measurements, matrix $\mathbf{B}=[\mathbf{B}_1|\mathbf{B}_2]$ is determined as

$$\mathbf{B} = \begin{bmatrix} 1 & 1 & 1 & 1 & 1 \\ 1 & 1 & 1 & -1 & 1 \\ 1 & 1 & 1 & 1 & -1 \\ 1 & 1 & 1 & -1 & -1 \end{bmatrix} \quad (27)$$

For each possible variation source ($f=1,\ldots,4$), and based on $\mathbf{C}_f$ and $\mathbf{B}$, the pdf is determined using Eq. (18)

Step 3: Determination of the likelihood functions. Using the

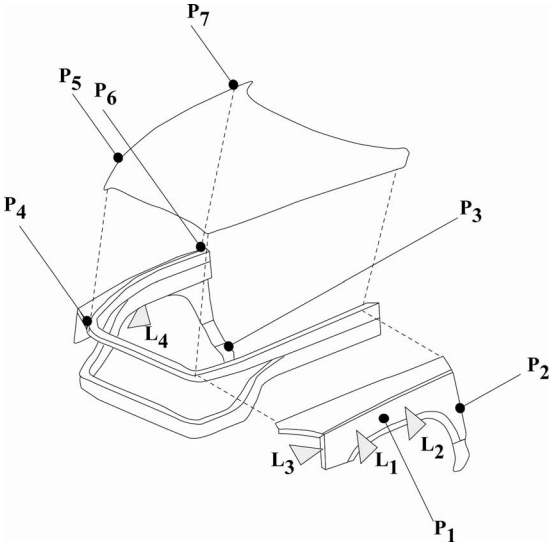

Fig. 9 Process parameters and measurements on the part

simulated data, the variance of the fault is estimated using Eq. (22) assuming that variance of the noise is known. Then, for each possible variation source ($f=1,\ldots,4$), the likelihood function $L^f(\mathbf{C}_f,\sigma_f^2,\sigma_\varepsilon^2)$ is calculated.

Step 4: Likelihood comparisons. For each possible variation source ($f=1,\ldots,4$), the likelihood ratios are determined for cases when only linear measurements are considered and when all measurements are considered simultaneously. When the ratio is negative, the corresponding fault is claimed to have happened in this system.

4.3 Variation Source Identification Results. For each simulation, 10,000 replications are performed. The results of the simulation for the relational measurements, are shown in Table 2. Table 2 shows the identification rate of the variation source. By identification, we understand the case when only the likelihood ratio corresponding to the fault that occurred is negative; in other words, the procedure can exactly pinpoint the specific fault that occurred in the system.

The variation source cannot be identified if only the linear measurements are used. Indeed, the system formed by matrix **A** is not diagnosable when only considering the linear measurements; in other words, the linear measurements do not contain enough information to the identification of all process faults [7,8]: The true variation source therefore can not be pointed out as the root cause of the dimension deviations of the product by only using linear measurements.

Table 2 Identification rates considering both linear and relational measurements

		Faulty locator L_1		
		S/N_0		
N	Noise	3 (%)	5 (%)	10 (%)
20	0.01	71.12	90.18	96.83
	0.05	81.25	97.63	99.97
	0.1	83.39	98.16	99.97
	0.2	86.85	98.89	99.98
50	0.01	85.75	98.15	99.84
	0.05	94.69	99.96	100
	0.1	95.89	99.97	100
	0.2	97.75	99.99	100
100	0.01	94.29	99.93	100
	0.05	99.11	100	100
	0.1	99.42	100	100
	0.2	99.77	100	100

On the other hand, as shown in Table 2, the variation source can be identified with different rates, given different scenarios, when using both linear and relational measurements. In the following, we discuss the different influential factors on the identification rate.

Clearly, from Table 2, the sample size affects the identification rate: As the sample size increases, the identification rate increases, given that all other parameters are kept constant. Similarly, from Table 2, as the signal-to-noise ratio increases, the identification rate increases. This result is expected since an increase in the signal-to-noise ratio corresponds to an increase of the importance of the fault signal over the perturbation in the measurement signals. Also, as the noise variance increases, the identification rate slightly increases. In fact, this can be explained by the fact that the signal-to-noise ratio is kept as constant. When the noise level increases and the signal-to-noise ratio does not change, the absolute difference between the fault variance and noise variance will increase and it will benefit the variance source identification procedure.

These simulation results can be used to develop heuristics based on the number of possible faults in the system, the parameters in the model, the noise level, and the expected variance shift of the faulty parameters. For the hood assembly example, with a sample size of 50, which is ten times the dimension of the measurement, and a signal-to-noise ratio larger than 5, the proposed variation source identification methodology provides a satisfactory performance.

5 Robustness Analysis

In order to make the problem analytically tractable and to gain useful insights, several assumptions are adopted in the derivation of this method. However, these assumed conditions might not be precisely met in practice. In this section, the robustness of the methodology is verified with respect to its assumptions using simulations based on the assembly process introduced in Sec. 4. First, the single fault assumption is relaxed, and a second weak variation source is introduced in the system. Then, the assumption of independence of the measurement noise with the fault is relaxed and the impact of correlation is studied. Finally, the assumption of normality of the fault is relaxed and the power of the methodology is measured as the distribution of the fault becomes less normal.

5.1 Presence of a Weak Variation Source in the System. In this paper, the occurrence of a single fault is defined as that instance when a single element in **u** (the random vector of the variation sources) has a large variance and is the major contributor to the product dimensional quality. In order to test the robustness of the methodology to the existence of a weak variation source, a new signal-to-noise (S/N_1) ratio is introduced corresponding to the ratio between the variance of the dominant variation source (S) and the variance of a weaker variation source (N_1). In this new simulation, the white noise level (N_0) is fixed and defined as 0.05. The results are shown in Table 3.

The trends shown in Table 3 are quite similar to those obtained when considering white noise only; thus, the methodology is shown to be robust. Other insights from Table 3 include the fact that the sample size has a quite significant impact on fault detection, and as sample size increases, the identification rate increases, given that all other parameters are kept constant. Similarly, as the signal-to-noise (S/N_1) ratio increases, the detection power increases. This is a clearly expected result, since it shows that as the

Table 3 Results considering an additional weak variation source

		Faulty locator L_1		
		S/N_1		
N	N_1	3 (%)	5 (%)	10 (%)
20	0.05	87.82	98.63	99.97
	0.1	91.47	98.63	99.95
	0.2	94.12	98.83	99.92
50	0.05	97.8	99.98	100
	0.1	99.02	99.98	100
	0.2	99.71	100	100
100	0.05	99.85	100	100
	0.1	99.99	100	100
	0.2	100	100	100

variance of the weak variation source gets weaker, i.e., as the dominant variation source gets stronger, the identification of the dominant variation source becomes easier.

5.2 Presence of Correlation Between Variation Source and Noise. Simulation has been performed in the presence of correlation between noise and variation source. In other words, the variables $\mathbf{u}$ and $\boldsymbol{\varepsilon}$ in the model have a generic covariance matrix

$$\boldsymbol{\Sigma} = \begin{bmatrix} \boldsymbol{\Sigma}_{\mathbf{u}} & \boldsymbol{\Sigma}_{\mathbf{u}\boldsymbol{\varepsilon}} \\ \boldsymbol{\Sigma}_{\mathbf{u}\boldsymbol{\varepsilon}} & \boldsymbol{\Sigma}_{\boldsymbol{\varepsilon}} \end{bmatrix}$$

where $\boldsymbol{\Sigma}_{\mathbf{u}}$ and $\boldsymbol{\Sigma}_{\varepsilon}$ are diagonal matrices and $\boldsymbol{\Sigma}_{\mathbf{u}\varepsilon}$ is constructed such that the correlation of the noise and variation source is controlled with a scalar parameter ρ_{ij}, where $\rho_{ij}=\sigma_{ij}/(\sigma_{ii}\sigma_{jj})$ is the correlation coefficient between fault i and measurement noise j. In the expression, σ_{ij} is the covariance between the ith variance source and the jth component of noise, and σ_{ii} and σ_{jj} are the standard deviation of the ith variance source and the jth component of noise, respectively. Simulation has been carried out for different correlation scenarios and correlation coefficients; as ρ_{ij} increases, the correlation between the variation source and the noise increases. The simulation is repeated 10,000 times for values of ρ_{ij} ranging from 0 to 0.3. The first two scenarios simulate the case where the fault is separately correlated with two different measurements. The third scenario is simulating the case where the fault is simultaneously correlated with two measurement noises. In all simulations, the other parameters of the simulation are kept constant: The signal to noise ratio is defined as 5 and the sample size is 50. The results are gathered in Table 4.

As shown with this simulation, the methodology performs well

Table 4 Results considering correlation

		Faulty locator L_1			
		ρ_{ij}			
(i,j)	N_0	0 (%)	0.1 (%)	0.2 (%)	0.3 (%)
L_1,ε_2	0.05	99.96	99.96	99.96	99.97
	0.2	99.99	99.99	99.99	99.99
L_1,ε_3	0.05	99.96	99.56	91.23	36.2
	0.2	99.99	99.79	94.16	43.3
$L_1,\varepsilon_2,\varepsilon_4$	0.05	99.96	99.95	99.95	99.95
	0.2	99.99	100	100	99.99

Table 5 Identification rate for Weibull distributed faults

	Faulty locator L_1		
	N		
Scale	20 (%)	50 (%)	100 (%)
0.1	92.19	99.66	99.99
2	99.80	100	100
3.4	99.99	100	100
5	99.96	100	100
8	98.37	99.99	100
10	78.44	91.98	98.46
12	48.98	53.96	58.22

in the presence of correlation; however, as expected, as the correlation increases, the methodology's detection power reduces. It can therefore be concluded that correlation disturbs the methodology negatively. The methodology is robust to this disturbance. One point worth pointing out is that the impact of the correlation is related not only to the magnitude of correlation, but also to the structure of the correlation. For example, Table 2 shows that the correlation does not have a significant impact on the identification rate when L_1 is correlated with ε_2 while it possesses a clear impact when L_1 is correlated with ε_3.

5.3 Impact of Non-Normally Distributed Faults. The robustness of the methodology when the faults are not normally distributed has been studied as well. The normality assumption for the faults is relaxed, and a Weibull distribution is used instead. The rational of selecting Weibull distribution is that the Weibull distribution has two parameters, one shape parameter and one scale parameter. When the scale parameter is equal to 3.4, the Weibull distribution behaves like a normal distribution. The shape parameter for the distribution is set to 0.5 and the scale parameter varies from 0.1 to 12. The simulation is repeated 10,000 times, and the variance of the white noise is kept constant at 0.05. The results are gathered in Table 5.

The results clearly show the robustness of the method to a relaxation of the normality assumption. Of course, the results in Table 5 show that the closer the distribution is to normal (scale parameter equals 3.4), the better the results.

6 Conclusion and Future Work

In this paper, we present a methodology for identifying variation sources in manufacturing processes including relational dimension measurements. The nonlinear measurements studied in this paper consist of the relative distance between two features. The proposed methodology is based on the explicit derivation of the pdf of the measurements, assuming that a single fault occurs in the system. The pdf is then used to conduct a series of comparisons between likelihood ratios to identify the process parameter at fault based on sampled measurements. This methodology is generic and can be applied to other nonlinear measurements than the distance between two features. If the joint pdf of the measurements cannot be obtained analytically, nonparametric methods of estimating joint probability functions can be used. A case study has been conducted to illustrate the effectiveness of the methodology. It has been demonstrated that including nonlinear relational measurements dramatically improves variation source identification capability. Also, in the case study, the influence of signal to noise ratios and sample sizes has been discussed. Furthermore, the robustness of the methodology to the relaxation of the key assumptions has been tested. The proposed methodology can be used for variation source identification using nonlinear relational measurements critical to product functionality.

The proposed methodology generates a new direction in diagnosis extending current state of the art to the use of relational

quality characteristics. Future extensions of this work include the study of other relations, leading to the inclusion of complicated measures such as form measures (flatness, circularity, and cylindricity) in variation source identification. Also, the method needs to be extended to scenarios when multiple faults occur. Finally, the study of the influence of a structured measurement noise could be investigated.

Acknowledgment

The authors gratefully acknowledge the financial support of the National Science Foundation Award Nos. CMMI-0529327, CMMI-0322147, and NSF-DMII-0239244, the NIST Advanced Technology Program ATP Cooperative Agreement No. 70NANB3H3054 and UK EPSRC Star Award. The authors also appreciate the fruitful discussion with Ramesh Kumar and Dr. Ying Zhou from Dimensional Control Systems, Inc.

References

[1] Ceglarek, D., and Shi, J., 1995, "Dimensional Variation Reduction for Automotive Body Assembly," Manuf. Rev., **8**, pp. 139–154.
[2] Ceglarek, D., and Shi, J., 1996, "Fixture Failure Diagnosis for the Autobody Assembly Using Pattern Recognition," ASME J. Eng. Ind., **118**(1), pp. 55–66.
[3] Ding, Y., Ceglarek, D., and Shi, J., 2002 "Fault Diagnosis of Multistage Manufacturing Processes by Using State Space Approach," ASME J. Manuf. Sci. Eng., **124**(2), pp. 313–322.
[4] Ceglarek, D., and Shi, J., 1999, "Fixture Failure Diagnosis for Sheet Metal Assembly With Consideration of Measurement Noise," ASME J. Manuf. Sci. Eng., **121**(4), pp. 771–777.
[5] Li, Z., Zhou, S., and Ding, Y., 2006, "Pattern Matching for Root Cause Identification of Manufacturing Processes With Consideration of General Structured Noise," IIE Trans., Qual. Reliab. Eng., **39**, pp. 251–263.
[6] Li, Z., and Zhou, S., 2006, "Robust Method of Multiple Variation Sources Identification in Manufacturing Processes for Quality Improvement," ASME J. Manuf. Sci. Eng., **128**(1), pp. 326–336.
[7] Ding, Y., Shi, J., and Ceglarek, D., 2002, "Diagnosability Analysis of Multistage Manufacturing Processes," ASME J. Dyn. Syst., Meas., Control, **124**(1), pp. 1–13.
[8] Zhou, S., Ding, Y., Chen, Y., and Shi, J., 2003, "Diagnosability Study of Multistage Manufacturing Processes Based on Linear Mixed-Effects Models," Technometrics, **45**(4), pp. 312–325.
[9] Zhou, S., Chen, Y., and Shi, J., 2004 "Root Cause Estimation and Statistical Testing for Quality Improvement of Multistage Manufacturing Processes," IEEE. Trans. Autom. Sci. Eng., **1**(1), pp. 73–83.
[10] Huang, Q., and Shi, J., 2004, "Variation Transmission Analysis and Diagnosis of Multi Operational Machining Processes," IIE Trans., **36**, pp. 807–815.
[11] Ding, Y., Zhou, S., and Chen, Y., 2005 "A Comparison of Process Variance Estimation Methods for In-process Dimensional Control," ASME J. Dyn. Syst., Meas., Control, **127**(1), pp. 69–79.
[12] Apley, D. W., and Shi, J., 2001, "A Factor-Analysis Method for Diagnosing Variability in Multistage Manufacturing Processes," Technometrics, **43**, pp. 84–95.
[13] Apley, D. W., and Lee, H. Y., 2003, "Identifying Spatial Variation Patterns in Multivariate Manufacturing Processes: A Blind Separation Approach," Technometrics, **45**(3), pp. 220–234.
[14] Jin, N., and Zhou, S., 2006, "Data-Driven Variation Source Identification of Manufacturing Processes Based on Eigenspace Comparison," Naval Res. Logistics Quart., **53**(5), pp. 383–396.
[15] Jin, N., and Zhou, S., 2006, "Signature Construction and Matching for Fault Diagnosis in Manufacturing Processes Through Fault Space Analysis," IIE Trans., **38**, pp. 341–354.
[16] American Society of Mechanical Engineers, Y14.5.1 Subcommittee, 1992, *Mathematization of Dimensioning and Tolerancing*, American Society of Mechanical Engineers, New York.
[17] Ding, Y., Ceglarek, D., and Shi, J., 2000, "Modeling and Diagnosis of Multistage Manufacturing Processes: Part I. State Space Model," in *Proceedings of the 2000 Japan/USA Symposium Flexible Automation*, Ann Arbor, MI.
[18] Apley, D. W., and Shi, J., 1998, "Diagnosis of Multiple Fixture Faults in Panel Assembly," ASME J. Manuf. Sci. Eng., **120**, pp. 793–801.
[19] Zhou, S., Huang, Y., and Shi, J., 2003, "State Space Modeling of Dimensional Variation Propagation in Multistage Machining Process Using Differential Motion Vectors," IEEE Trans. Rob. Autom., **19**, pp. 296–309.
[20] Montgomery, D. C., 2001, *Introduction to Statistical Quality Control*, 4th ed., Wiley, New York.
[21] Lehmann, E. L., 1986, *Testing Statistical Hypotheses*, 2nd ed. Wiley, New York.
[22] Neyman, J., and Pearson, E. S., 1933, "On the Problem of the Most Efficient Tests of Statistical Hypotheses," Philos. Trans. R. Soc. London, Ser. A, **231**, pp. 289–337.
[23] Djurdjanovic, D., and Ni, J., 2001, "Linear State Space Modeling of Dimensional Machining Errors," Trans. North Am. Manuf. Res. Inst. SME, **29**, pp. 541–548.
[24] Huang, Q., Zhou, N., and Shi, J., 2000, "Stream of Variation Modeling and Diagnosis of Multi-Station Machining Processes," in *Proceedings of the 2000 ASME International Mechanical Engineering Congress Expo (IMECE'00)*, Orlando, FL, pp. 81–88.
[25] Jin, J., and Shi, J., 1999, "State Space Modeling of Sheet Metal Assembly for Dimensional Control," ASME J. Manuf. Sci. Eng., **121**, pp. 756–762.
[26] Loose, J.-P., Zhou, S., and Ceglarek, D., 2007, "Kinematic Analysis of Dimensional Variation Propagation for Multistage Machining Processes With General Fixture Layout," IEEE. Trans. Autom. Sci. Eng., **4**(2), pp. 141–152.
[27] Mantripragada, R., and Whitney, D. E., 1999, "Modeling and Controlling Variation Propagation in Mechanical Assemblies Using State Transition Models," IEEE Trans. Rob. Autom., **15**, pp. 124–140.
[28] Ceglarek, D., Shi, J., and Wu, S. M., 1994, "A Knowledge-Based Diagnosis Approach for the Launch of the Auto-Body Assembly Process," ASME J. Eng. Ind., **116**(4), pp. 491–499.
[29] Ceglarek, D., Huang, W., Zhou, S., Ding, Y., Kumar, R., and Zhou, Y., 2004, "Time-Based Competition in Manufacturing: Stream-of-Variation Analysis (SOVA) Methodology-Review," Int. J. Flexible Manufacturing Systems, **16**(1), pp. 11–44.